Theoretical study of Axion-Like Particle (ALP) couplings to quarks and gluons, and experimental study of ALP resonances in dijet invariant mass spectrum using Monte Carlo data

Komal Tauqeer
Quaid-i-Azam University,
Islamabad, Pakistan

November 1, 2019

Abstract

Axion-like particles are hypothetical particles which are well motivated in many Beyond Standard Model (BSM) models. They are singlets under the Standard Model (SM) gauge group and one can describe their interactions with SM fields by an effective Lagrangian. In this report, we will discuss the interactions of ALPs to the SM particles specifically quarks and gluons. At the partonic level, the pseudoscalar ALP can decay into colored particles. At tree-level the relevant modes are $a \to gg$ and $a \to q\bar{q}$. We will be looking for ALP resonances with mass 10 GeV, 80 GeV and 350 GeV. We will present the study of ALP decay widths as a function of ALP mass and coupling strength. Also we discuss the expected cross sections for various processes having ALPs as mediator particle with quarks and gluons as a initial and final state particles. Furthermore, we present phenomenological study of resonances decaying into two jets, called "dijet events" using simulated Monte Carlo (MC) data. We will discuss in detail the study of parton level, particle level and detector level widths of an ALP with mass 80 GeV and 350 GeV by analyzing the dijet invariant mass distribution. Finally, we will summarize the relative widths for each case.

1 Introduction

The Higgs boson discovery in 2012 was an incredible success of particle physics in the quest of understanding the constituents of matter within the Standard Model. This discovery has opened up new paths for the discovery of new particles with potential to find new physics. The Standard Model is not complete because it does not give answers to many mysteries such as the origin of Dark matter and Dark energy etc. Furthermore, the Standard Model does not provides predictions or reasons for many of its parameters. It is therefore essential to look for BSM physics to find answers to such questions. Low mass and weakly interacting particles are often found in extensions of SM, Axions and Axion-like particles (ALPs) are prime examples of such particles [1] [2]. Axions are a direct consequence of the Peccei-Quinn solution to the strong Charge-Parity (CP) problem in Quantum Chromo Dynamics (QCD) [3]. Many new models predict that such new particles have very feeble interactions with ordinary matter, which typically results from underlying new dynamics at energy scales much larger than the electroweak scale. Therefore, searching for presence of such particles opens a new window towards the understanding of the underlying structure of fundamental physics.

2 Theoretical Motivation

The charge conjugation and parity are conserved in the electromagnetic and strong interactions, and it seems to be violated in weak interactions [4]. The most general vacuum of QCD can have a term that violates CP symmetry, but in experiments no evidence has been observed that shows CP violation in the strong interaction. This problem is referred as the “strong CP problem”. A well-known proposed solution to this problem involves a new pseudoscalar particle, the Axion. The Peccei–Quinn theory predicts that the θ parameter of the QCD Lagrangian is a dynamic field rather than a constant value. This idea comes from the fact that particles arises from disturbances in the quantum fields. The potential of this dynamic field naturally cancels the effect of the θ parameter. Axions are the massless Goldstone bosons of the spontaneously broken Peccei-Quinn Symmetry at a high energy scale of the Axionic field [5]. Discovering Axions is thus a way to find out whether the Peccei-Quinn Symmetry is a real symmetry of nature or not. For most of the experimental searches, the key parameters of these Axion are it’s mass and it’s coupling to photons. Originally it was assumed that the symmetry breaking scale must be close to the weak scale ($\approx$ 246 GeV) but the collider experiments have excluded this possibility by restricting the scale to be larger than 10^5 GeV [6]. Since the axion mass is inversely proportional to energy scale, a higher energy scale means a lower axion mass. Similarly the couplings, being inversely proportional to the energy scale, must have small values. Hence Axions are expected to have low mass and weak interactions. This makes them a promising candidate for probing new physics in high-precision low-energy experiments.

3 Effective Lagrangian for ALPs

As discussed in the previous section, the mass of ALP or Axion m_a is assumed to be smaller than the electroweak scale. The most general effective Lagrangian for Axions reads as [7]

$$\mathscr{L}_{eff}{}^{D\leq 5} = \frac{1}{2}(\partial_\mu a)(\partial^\mu a) - \frac{m_{a,0}^2}{2}a^2 + \frac{\partial^\mu a}{\Lambda}\sum_F \bar{\psi}_F \boldsymbol{C}_F \gamma_\mu \psi_F + g_s^2 C_{GG}\frac{a}{\Lambda}G_{\mu\nu}^A \tilde{G}^{\mu\nu,A} \tag{1}$$

$$+g^2 C_{WW}\frac{a}{\Lambda}W_{\mu\nu}^A \tilde{W}^{\mu\nu,A} + g\prime^2 C_{BB}\frac{a}{\Lambda}B_{\mu\nu}\tilde{B}^{\mu\nu}$$

where $G_{\mu\nu}^A$, $W_{\mu\nu}^A$, $B_{\mu\nu}$ are the field strength tensors of $SU(3)_c$, $SU(2)_L$, $U(1)_Y$ and g_s, g, g' denote the corresponding coupling constant and Λ is the symmetry breaking scale. The dual field strength tensors are defined as $\tilde{B}^{\mu\nu} = \frac{1}{2}\epsilon^{\mu\nu\alpha\beta}B_{\alpha\beta}$.

The first term $\frac{1}{2}(\partial_\mu a)(\partial^\mu a)$ in Lagrangian is the kinetic energy term of the Axionic field. The second term $\frac{m_{a,0}^2}{2}a^2$ is the mass term for the Axion. The term $\frac{\partial^\mu a}{\Lambda}\sum_F \bar{\psi}_F \boldsymbol{C}_F \gamma_\mu \psi_F$ describes the interactions between Axion and fermions. $g_s^2 C_{GG}\frac{a}{\Lambda}G_{\mu\nu}^A \tilde{G}^{\mu\nu,A}$, $g^2 C_{WW}\frac{a}{\Lambda}W_{\mu\nu}^A \tilde{W}^{\mu\nu,A}$ and $g\prime^2 C_{BB}\frac{a}{\Lambda}B_{\mu\nu}\tilde{B}^{\mu\nu}$ describes the couplings between the vector bosons of the SM.

4 ALP decays to SM particles

This effective Lagrangian (1) governs the leading interactions (in powers of $(\frac{v}{\Lambda})$) giving rise to ALP decays into pairs of SM gauge bosons and fermions. We will study the tree-level interactions of ALPs with SM particles specifically quarks and gluons.

10 GeV	80 GeV	350 GeV
0.179	0.121	0.099

Table 1: Values of α_s as a function of m_a

4.1 ALP decays to Hadrons

At the partonic level, the pseudoscalar Alp can decay into colored particles. At tree-level the most relevant modes are $a \rightarrow gg$ and $a \rightarrow q\bar{q}$. The decay rate of ALP going to hadrons is given by [7]

$$\Gamma(a \rightarrow hadrons) = \frac{32\pi\alpha_s^2(m_a)m_a^3}{\Lambda^2}[1+(\frac{97}{4}-\frac{7n_q}{6})\frac{\alpha_s(m_a)}{\pi}] \mid C_{GG}+\sum_{q=1}^{n_q}\frac{C_{qq}}{32\pi^2} \mid^2$$
$$\equiv \frac{32\pi\alpha_s^2(m_a)m_a^3}{\Lambda^2}[1+\frac{83}{4}\frac{\alpha_s(m_a)}{\pi}] \mid C_{GG}^{eff} \mid^2 \quad (2)$$

where $n_q = 3$ is the number of light quark flavours and α_s is the coupling strength of strong interaction (QCD) as a function of ALP mass. Its values for different ALP masses is summarized in Table 1. For simplicity we will choose $n_q = 1$ i.e. only "up type" quarks for this study. To a good approximation this rate scales with the third power of the ALP mass.

5 Theoretical calculation of ALP decay widths

In this section, we will discuss ALP decay widths into SM quarks and gluons using eq. (2) specifically looking at three different mass points and with varying coupling strengths. Table 2 below shows the decay rates for 10 GeV, 80 GeV and 350 GeV Alp mass. The C++ code implementing eq. (2) can be found in the GitHub repository [8]. On the basis of this calculation we can conclude that the quark couplings can be neglected safely (see section 7).

6 Calculation of Decay widths of ALP using MadGraph5_aMC@NLO

In order to verify theoretically calculated decay rates using eq. (2), we have also calculated the decay rates of same processes using MadGraph5. For this

Case	**10 GeV**	**80 GeV**	**350 GeV**
$a \to gg, C_G = 1$	0.00744232 GeV	1.42118 GeV	72.8637 GeV
$a \to gg, C_G = \frac{1}{4\pi}$	4.76309e-05 GeV	0.00909555 GeV	0.466327 GeV
$a \to q\bar{q}, C_{qq} = 1$	5.77732e-12 GeV	4.62186e-11 GeV	2.02206e-10 GeV

Table 2: ALP decay rates

purpose we have used a model file which implements effective Lagrangain [1]. The summary of decay widths calculated in this manner is shown in Table 3 below. The compatibility of the theory prediction with Madgraph5 will be discussed in the next section.

Case	**10 GeV**	**80 GeV**	**350 GeV**
$a \to gg, C_G = 1$	0.003214 GeV	0.751 GeV	41.77 GeV
$a \to gg, C_G = \frac{1}{4\pi}$	2.035e-05 GeV	0.004756 GeV	0.2645 GeV
$a \to q\bar{q}, C_{qq} = 1$	7.762e-13 GeV	7.762e-12 GeV	6.209e-11 GeV

Table 3: ALP decay rates using MadGraph5

7 Comparison between theory and MadGraph5 calculated decay widths

To make a comparison plot between the theoretical and MadGraph5 calculated decay widths, we used the python code in GitHub repository [9]. The plot shown below reveals good agreement between theory and Monte Carlo. Also, we can see from the plot that ALP decay width to gluons is much greater than the quarks. This enables us to conclude that the majority of the times ALP will decay into gluons rather than quarks and we can neglect quark decays in the following study.

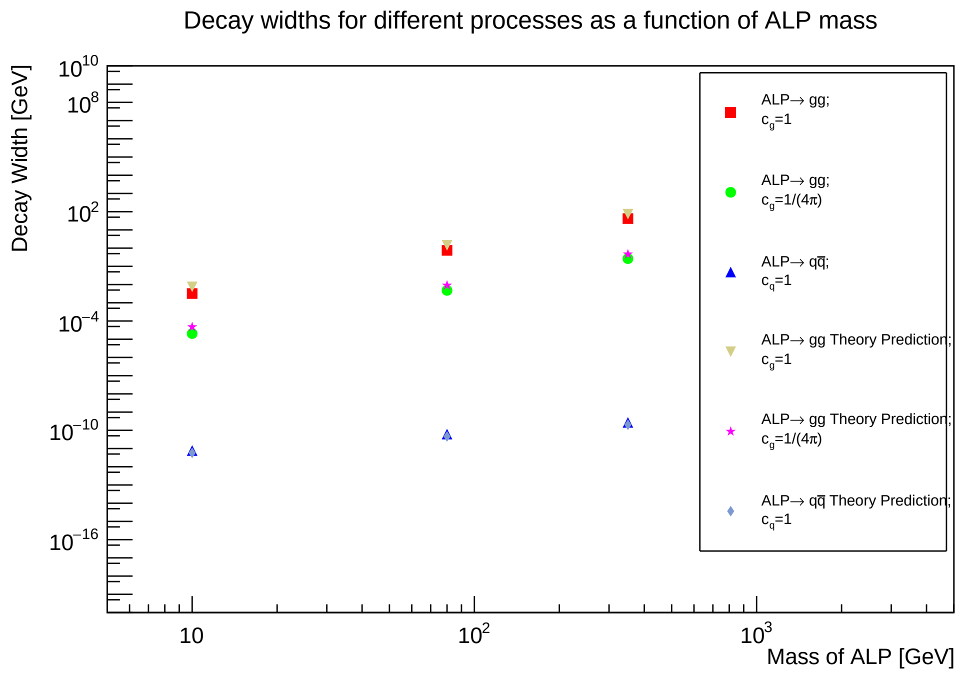

Figure 1: ALP decay widths

8 Branching Ratios

Using the calculated decay widths from MadGraph, we have also calculated ALP branching ratios. Summary is given in the tables below.

Case	BR formulla	10 GeV	80 GeV	350 GeV
$a \to gg, C_G = 1$	$\Gamma(ALP \to gg)/\Gamma_{tot}(ALP)$	0.99597	0.9990	0.94161
$a \to gg, C_G = \frac{1}{4\pi}$	$\Gamma(ALP \to gg)/\Gamma_{tot}(ALP)$	0.006306	0.00632	0.005962
$a \to q\bar{q}, C_{qq} = 1$	$\Gamma(ALP \to q\bar{q})/\Gamma_{tot}(ALP)$	2.4053e-09	8.2599e-11	6.1248e-12

Table 4: Branching ratios

9 Expected cross-section for the processes involving ALP, quarks and gluons

In this section, we will present cross-sections for the possible processes where ALP can couple to gluons and quarks. Feynman diagrams for such processes are shown in the figure below.

Figure 2: Feynman diagrams

Case	10 GeV	80 GeV	350 GeV
$gg \to a \to gg; C_G = 1$	1.048e+07 pb	6.319e+05 pb	2.471e+04 pb
$gg \to a \to gg; C_G = \frac{1}{4\pi}$	6.625e+04 pb	4024 pb	161.9 pb
$gg \to a \to q\bar{q}; C_G = 1; C_{qq} = 1$	0.0188 pb	4.278e-05 pb	1.337e-07 pb
$gg \to a \to q\bar{q}; C_G = \frac{1}{4\pi}; C_{qq} = 1$	0.01721 pb	4.278e-05 pb	7.627e-08 pb
$q\bar{q} \to a \to gg; C_G = 1; C_{qq} = 1$	0.0001495 pb	1.233e-06 pb	1.333e-08 pb
$q\bar{q} \to a \to gg; C_G = \frac{1}{4\pi}; C_{qq} = 1$	0.0001372 pb	1.231e-06 pb	7.583e-09 pb
$q\bar{q} \to a \to q\bar{q}; C_{qq} = 1$	4.631e-10 pb	4.121e-12 pb	1.44e-17 pb

Table 5: ALP Cross-sections

9.1 Summary plot for cross-sections

To summarize above cross-sections for various processes and varying coupling values we have a summary plot to show, see figure 3 (for python code for making this plot see [10]. It can be clearly seen that the ALP branching ratios to gluons is much greater than the quarks, therefore the cross section for $gg \to a \to gg$ is much greater than $q\bar{q} \to a \to q\bar{q}$.

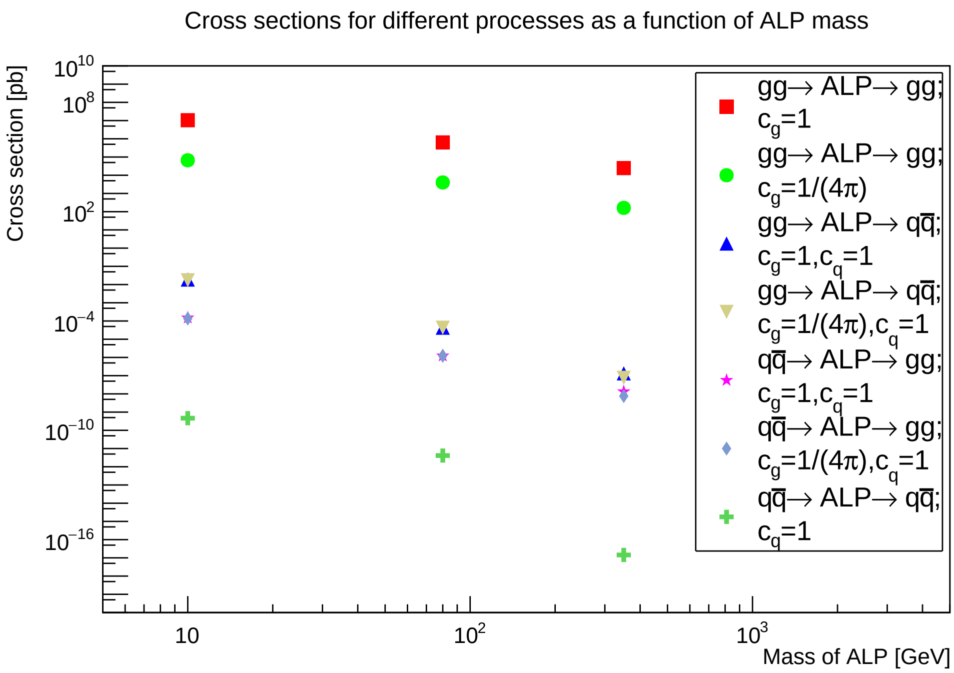

Figure 3: Cross-sections of processes including ALP, gluons and quarks

10 Search for ALP resonances in dijet mass distributions

In this section we will discuss the Alp resonance in the invariant mass spectrum at three levels: parton, particle and detector level. We will discuss how such resonances broadens at each level, using Simulated data. For this section we will only look for the process $gg \to a \to gg; C_G = 1$ because this process has the highest cross-section amongst the rest discussed in the previous section.

10.1 Event generation

The simulated Monte Carlo events are generated using MadGraph5 using model file that implements eq. (1). 10,000 dijet events were generated for the process $gg \to a \to gg; C_G = 1$ for 80 GeV and 350 GeV ALP at both generator level and detector level. At generator level, the parton-parton interactions are done in MadGraph5 and at particle level, parton showering is done using PYTHIA8 as shown in figure 4. At the detector level, particle matter interactions are done using Delphes.

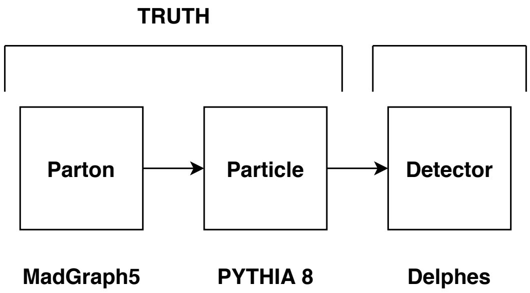

Figure 4: The different steps of generating events (taken from [11])

10.2 Invariant mass distributions

In order to analyse Simulated events, MadAnalysis5 was used. For details of the MadAnalysis5 framework, see the GitHub repository [12]. We will now present the dijet invariant mass spectrum for an ALP resonance at each level. Only first two leading partons(for parton level) or jets (for particle and detector level) in P_T are used to calculate invariant mass using the formula

$$M^2 = 2P_{T_1}P_{T_2}(cosh(\eta_1 - \eta_2) - cos(\phi_1 - \phi_2))$$

10.2.1 Parton-Level distributions

In order to calculate mass of resonance at parton level 4-momenta of the partons were used. Only the leading two partons in P_T were selected to calculate the invariant mass. The invariant mass spectrum was then fitted with the bukin function.

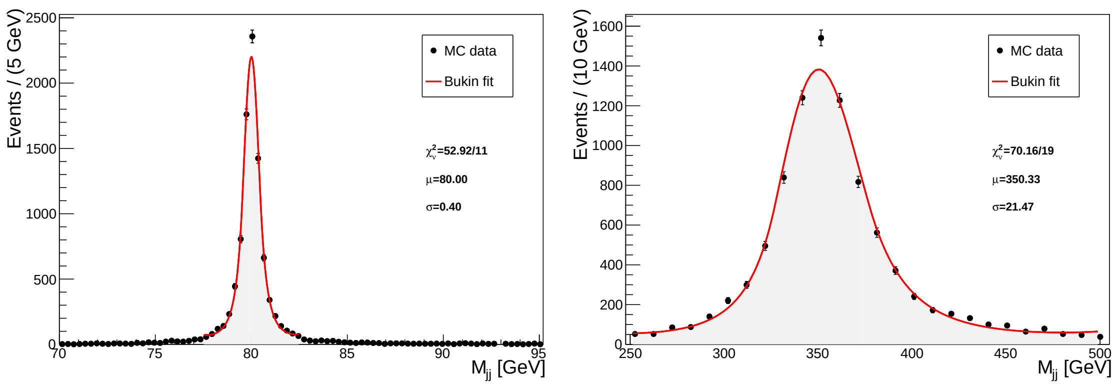

Figure 5: Parton level dijet invariant mass distributions for 80 GeV and 350 GeV ALP.

10.2.2 Particle-Level distributions

Due to parton showering, we expect to see a smearing effect in the resonance peak at particle level. For parton showering we have used PYTHIA8. The resulting event files were reconstructed by anti-k_t algorithm using FastJet simulation requiring $R = 0.4$. Only the leading two reconstructed jets in P_T were selected to calculate invariant mass. Finally, we fit the distribution with the bukin function.

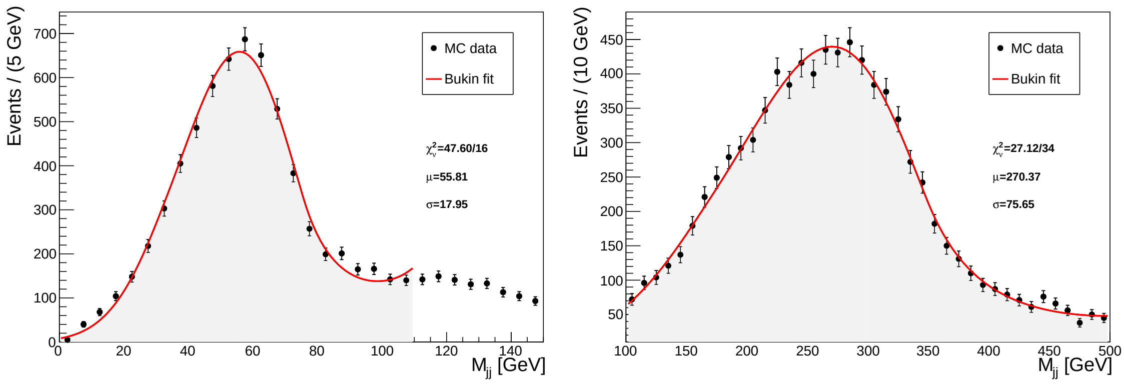

Figure 6: Particle level dijet invariant mass distributions for 80 GeV and 350 GeV ALP.

10.2.3 Detector-Level distributions

At detector level, measurement of the particles will result in further broadening of the peaks due to the simulated interaction of particles with the detector matter. For detector simulation and reconstruction we have used Delphes on the MC samples generated by MadGraph5 at parton level,pythia for showering and the resulting delphes root files were further analysed in the expert mode of MadAnalysis5. Only the leading two reconstructed jets in P_T were selected to calculate the invariant mass. Bukin function was used to fit the distribution.

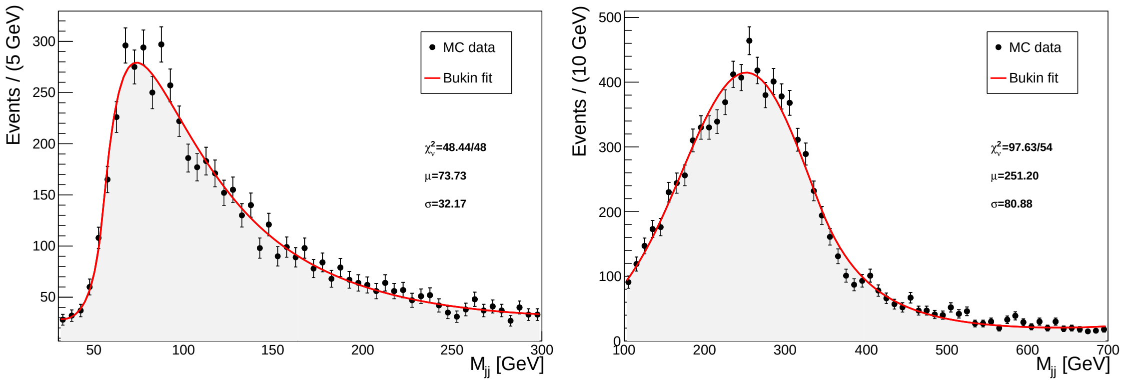

Figure 7: Detector level dijet invariant mass distributions for 80 GeV and 350 GeV ALP.

10.3 Relative widths for $gg \to a \to gg; C_G = 1$

Table 18 summarizes the relative widths of ALP resonance at all three levels and a comparison has been performed with the relative widths calculated from theory.

It is important to note the difference between the values of relative width at each level. The parton level distribution being narrower has relatively smaller RMS/Mean ratio. When we include parton showering effect at particle level, we expect our dijet invariant mass spectrum to get broader, hence RMS/Mean ratio increases. Upon simulating the interaction of particles with detector matter, we expect further smearing in the energy distribution which causes further increase in the value of RMS/Mean at the detector level.

Mass	**Parton Level** RMS/Mean	**Particle level** RMS/Mean	**Detector level** RMS/Mean	**Theory** Width/Mass
80	0.45/80 = 0.0056	16.89/57.7 = 0.29	30.8/74.2 = 0.42	1.42/80 = 0.018
350	84.8/371.5 = 0.23	75.6/270.4 = 0.28	80/251 = 0.32	72.9/350 = 0.21

Table 6: Relative widths for $gg \to a \to gg; C_G = 1$

11 Conclusions

In this report, we have summarized a study of the interaction of Axions with gluons and quarks. Axions can couple to both gluons and quarks, however their coupling to gluons is many orders of magnitude greater than quarks. Also we have discussed, using simulated data, how the ALP resonance peak in dijet mass spectrum broadens from parton level to detector level. This is mainly due to the fact that we can not measure particles in detector with full accuracy. Also when we take into account hadronization and particle interactions with matter we expect the invariant mass peak to be broader than parton level.

In order to detect new particles like Axions in real data with huge background, it is important to study well their resonance peaks at MC level and devise ways to detect them in the real data by constraining the large QCD background.

References

[1] Steven Weinberg. A new light boson? URL:`https://link.aps.org/doi/10.1103/PhysRevLett.40.223`, Jan 1978.

[2] Andreas Ringwald. Axions and axion-like particles. *arXiv preprint arXiv:1407.0546*, 2014.

[3] R.D. Peccei and Helen Quinn. Cp conservation in the presence of pseudoparticles. *Physical Review Letters - PHYS REV LETT*, 38:1440–1443, 06 1977.

[4] A. Buras. CP violation in electroweak interactions, 2015. revision #151973.

[5] F. Wilczek. Problem of strong p and t invariance in the presence of instantons. URL:`https://link.aps.org/doi/10.1103/PhysRevLett.40.279`, Jan 1978.

[6] K. Baker, G. Cantatore, S. A. Cetin, M. Davenport, K. Desch, B. Döbrich, H. Gies, I. G. Irastorza, J. Jaeckel, A. Lindner, and et al. The quest for axions and other new light particles. URL:http://dx.doi.org/10.1002/andp.201300727, Jun 2013.

[7] Martin Bauer, Matthias Neubert, and Andrea Thamm. Collider probes of axion-like particles. URL:http://dx.doi.org/10.1007/JHEP12(2017)044, Dec 2017.

[8] Komal Tauqeer. C++ code implemting eq.(2). URL:https://github.com/KomalTauqeer/ALP_theory_calculation/blob/master/decayRateALPuu.c, 2019.

[9] Komal Tauqeer. Python code for plotting fig. 1. URL:https://github.com/KomalTauqeer/ALP_theory_calculation/blob/master/WidthSummaryPlot.py, 2019.

[10] Komal Tauqeer. Python code for plotting fig. 3. URL:https://github.com/KomalTauqeer/ALP_theory_calculation/blob/master/CrossSectionSummaryPlot.py, 2019.

[11] Martin Angelsmark. Studies of dark matter signals at the lhc, 2017. Student Paper.

[12] Komal Tauqeer. Madanalysis5 framework. URL:https://github.com/KomalTauqeer/madanalysis5_ALP, 2019.